Engineering Structures 32 (2010) 2596–2605

Contents lists available at ScienceDirect

Engineering Structures

journal homepage: www.elsevier.com/locate/engstruct

Time-variant service reliability of post-tensioned, segmental, concrete bridges exposed to corrosive environments

R.G. Pillai [a,*], M.D. Hueste [a], P. Gardoni [a], D. Trejo [b], K.F. Reinschmidt [a]

[a] Zachry Department of Civil Engineering, Texas A&M University, College Station, TX, USA
[b] Department of Civil and Construction Engineering, Oregon State University, Corvallis, OR, USA

ARTICLE INFO

Article history:
Received 20 August 2009
Received in revised form
22 December 2009
Accepted 25 April 2010
Available online 15 June 2010

Keywords:
Segmental
Post-tensioned
Prestressed concrete
Bridge
Tendon
Strand
Void
Corrosion
Normal stress
Serviceability
Reliability

ABSTRACT

This paper presents a framework for assessing the service reliability of post-tensioned (PT) bridges with damaged and undamaged tendons containing voids, chlorides, and moisture. The service reliability is defined based on the probability that the normal stress due to the applied loads (i.e., demand) at the midspan of the girder attains or exceeds the corresponding allowable normal stress (i.e., capacity). The probabilistic model to determine the normal stress demand is formulated using statistical characteristics of highway traffic and bridge design loads, probabilistic models for the tension capacity of corroding strands, the AASHTO LRFD stress model for strands, and Todeschini's nonlinear stress model for concrete. The probabilistic model for capacity is based on the AASHTO LRFD normal stress limits. Using the developed reliability framework and Monte Carlo simulation, the time-variant service reliability of a typical PT bridge over a 75-year period is estimated. After chloride and moisture infiltrate the tendons, the service reliability reduces to a value below recommended values within a relatively short period of time.

1. Introduction

The presence of chlorides, moisture, damage, and voids has been observed in tendon systems in segmental post-tensioned (PT) bridges. These conditions can lead to accelerated corrosion of strands resulting in tendon failure. For example, the Niles Channel, Mid-bay, and Bob Graham Sunshine Skyway bridges in Florida, and the Varina-Enon bridge in Virginia experienced tendon failures [1–4]. These incidents raise concern over the safety and serviceability of PT bridges exposed to corrosive environments.

The generalized reliability index, β can be considered as a quantitative measure for the safety (if the strength limit state is considered) or serviceability (if the service limit state is considered) of structural systems. In general, the term β can be defined based on the probability of the occurrence of failures (strength or service failure). To ensure good safety or serviceability, the value of β corresponding to a chosen limit state must be greater than a minimum required value, defined as the target reliability index, β_{target}. To ensure acceptable levels of safety, the load and resistance factors for the strength limit states in the American Association of State Highway and Transportation Officials, Load Resistance Factor Design (AASHTO LRFD) Specifications [5] are calibrated for a β_{target}, of 3.5 [6]. However, the load and resistance factors for the service limit states in AASHTO LRFD Specifications [5] are not yet calibrated for a specific β_{target}. Based on a comparative study on the reliability of concrete girders assessed using the AASHTO LRFD Specifications [7], Chinese code [8], and Hong Kong code [9], Du and Au [10] recommended to calibrate the bridge design codes for service limit states, to ensure a high level of serviceability. At present, the National Cooperative Highway Research Program (NCHRP) is conducting an unpublished study [11] on the calibration of the AASHTO LRFD Specifications for service limit states.

Researchers have suggested various β_{target} values to improve service reliability. A β_{target} value between 1.6 and 2.0 has been suggested for structural steel members [12]. A β_{target} value of 2.0 has been suggested for timber beams [13,14] and reinforced concrete beams [15]. The above discussion indicates that the typical β_{target} value for service failure is smaller than that for strength failure. This is because the consequences of service failure (e.g. tendon failure) are more affordable than the consequences of

* Corresponding author. Tel.: +1 979 575 9524; fax: +1 979 845 6554.
E-mail address: radhakpg@yahoo.com (R.G. Pillai).

0141-0296/$ – see front matter © 2010 Elsevier Ltd. All rights reserved.
doi:10.1016/j.engstruct.2010.04.032

Nomenclature

β	Reliability index
β_{target}	Target reliability index
$\beta(\mathbf{x}, t)$	Time-variant reliability index
Δf_{pLT}	Prestress loss due to long term effects
ε	Standard normal random variable, $\sim$N(0, 1)
ϕ	Curvature at midspan of the girder
ϕ_{wet}	Wet-time (in months) in a year divided by 12
γ_{load}	Load factor
ρ_{box}	Unit weight of concrete in box section
$\rho_{\text{non-box}}$	Unit weight of concrete in overlay, wearing surface, and side barriers
θ_i	Unknown model parameter
σ	Standard deviation of model error
$A_{\text{as-received}}$	Cross-sectional area of as-received strand
A_c	Area of the concrete cross section
c	Depth of neutral axis at midspan of the girder
c_b	Distance from centroid of concrete cross-section to extreme bottom fiber
c_t	Distance from centroid of concrete cross-section to extreme top fiber
CG	Center of gravity
C_M	Moment capacity
C_f	Stress capacity
$C_{\text{compression},1}$	Allowable compressive stress at top fiber due to dead load only
$C_{\text{compression},2}$	Allowable compressive stress at top fiber due to dead and live loads
C_{tension}	Allowable compressive stress at top fiber due to dead and live loads
COV	Coefficient of Variation
C_T	Tension capacity
$C_{T,\text{as-received}}$	Tension capacity of as-received strand
DL_{box}	Dead load due to precast concrete box section
$DL_{\text{non-box}}$	Dead load due to concrete overlay, wearing surface, and side barriers
D_M	Moment demand
$D_{M,DL}$	Moment demand due to dead load only
$D_{M,LL}$	Moment demand due to live and impact loads
D_f	Stress capacity
$D_{\text{compression},1}$	Applied compressive stress at top fiber due to dead load only
$D_{\text{compression},2}$	Applied compressive stress at top fiber due to dead and live loads
D_{tension}	Applied compressive stress at top fiber due to dead and live loads
e_j	Eccentricity of jth strand from the centroid of concrete cross section
E_c	Elastic modulus of concrete
f_c	Normal compressive stress in concrete
f'_c	Actual compressive strength of concrete
$f'_{c,\text{specified}}$	Specified compressive strength of concrete
f_{pe}	Effective prestress in strand
f_{pi}	Initial prestress after anchoring
f_{ps}	Total stress in prestressing strand
f_{py}	Yield strength of prestressing strand
f_{pu}	Ultimate tensile strength of strand
F	Normal force in concrete
F_C	Normal compressive force
F_T	Normal tensile force
$g(\mathbf{x}, t)$	Service limit state function
$h_{t_{CA}}$	$\frac{\text{Total atmospheric exposure time (years)}}{\text{standardizing factor}} = \frac{t_{CA}}{0.75}$
n_{CA}	Constant based on field information $= -0.005$
h_T	Ambient exposure temperature (°F) $= T$ (°F)
h_{RH}	$\frac{\text{Ambient relative humidity (\%)}}{\text{Maximum Relative humidity (\%)}} = \frac{RH\ (\%)}{100}$
$h_{\%gCl^-}$	$\frac{\%Cl^-\text{ in the grout (by weight)}}{\%sCl^-_{\text{saturated chloride solution}}} = \frac{\%gCl^-}{35.7}$
$h_{\%sCl^-}$	$\frac{\%Cl^-\text{ in the water inside the tendon}}{\%sCl^-_{\text{saturated chloride solution}}} = \frac{\%sCl^-}{35.7}$
$h_{t_{WD}}$	$\phi_{\text{wet}} \times$ Total exposure time (years) $= \phi_{\text{wet}} \times t_{WD}$
j	Subscript j indicates jth strand
k	Moment arm
l_e	Effective tendon length (inches)
l_i	Length of the strand between anchorages (inches)
LL_{lane}	Live load based on lane load
LL_{tandem}	Live load based on tandem load
LL_{truck}	Live load based on truck load
M	Bending moment
MUTS	Minimum ultimate tensile strength
N_s	Number of support hinges crossed by the strand between the anchorages
N_{strands}	Total number of strands in the cross section
P_f	Probability of service failure
$P_{f,\text{target}}$	Target probability of service failure
$P_{\text{loss,as-received}}$	Prestress loss in as-received strands
PT	Post-tensioned
r	Radius of gyration
RH	Relative Humidity
S^t	Section modulus of concrete section w.r.t. the extreme top fiber
S_b	Section modulus of concrete section w.r.t. the extreme bottom fiber
T	Temperature
t	Exposure time or age of bridge
$\mathbf{x}$	Vector of influential parameters and variables
WDT	Number of tendons with wet–dry exposure

a strength failure (e.g., bridge collapse). The designation 13822, *Bases for design of structures — Assessment of existing structures* by the International Organization of Standardization (ISO 2001) recommends β_{target} values of 0 and 1.5 for service failures with reversible and irreversible consequences of failures, respectively.

The reliability of a structural system can reduce as a function of exposure conditions and time. Pillai et al. [16] developed a framework to assess the time-variant strength or flexural reliability (i.e., a safety performance indicator) of PT bridges exposed to corrosive environments. A framework to assess the time-variant service reliability is needed to assess the serviceability issues of PT bridges exposed to corrosive environments. These serviceability issues include concrete cracking, inelastic concrete compression, and strand/tendon failure due to corrosion and/or excessive normal stresses.

A general basis for the definition of β was provided earlier in this paper. Herein, the term β is defined based on the probability that the normal stress due to the applied loads (i.e., normal stress demand, D_f) at the midspan of the girder attains or exceeds the corresponding allowable normal stress (i.e., normal stress capacity, C_f). Based on structural reliability techniques and probabilistic models for D_f and C_f, this paper develops a framework to assess the time-variant service reliability index, $\beta(\mathbf{x}, t)$, of PT bridges. The vector $\mathbf{x}$ indicates the set of parameters and random variables (i.e., the tension capacity (denoted as C_T) of strands, the void condition, damage condition, environmental condition of tendons, and the external loading conditions and geometrical, material, and structural characteristics of the bridge) influencing D_f and C_f. The term t indicates the exposure time. Herein, 'service reliability' is simply denoted as 'reliability'.

The remaining paper is organized as follows. First, a review on corrosion and applied normal stresses in PT bridges is provided.

Then, a general framework to determine $\beta(\mathbf{x}, t)$ is presented. Then the framework for probabilistic estimations of C_f and D_f are discussed. A discussion on the random variables used in the framework for estimating C_f and D_f is then described. Following this, using an application of the developed reliability framework, the values of $\beta(\mathbf{x}, t)$ for a typical PT bridge are determined based on a set of random variables and a pre-defined set of parameter combinations (i.e., $\mathbf{x}$ and t). Finally, the conclusions from this study are provided. Further details on this research can be obtained from [17].

2. Corrosion and applied normal stresses in post-tensioned bridges

2.1. Exposure conditions and corrosion mechanisms

A tendon that is placed outside the concrete and within the walls of the box is defined as an external tendon. A tendon that is placed inside the concrete of the box girder is defined as an internal tendon. This paper focuses on the corrosion of external tendons only and its effect on $\beta(\mathbf{x}, t)$. The presence of damage and openings in external tendons, along with voids, chlorides, and moisture inside these tendons and anchorage zones can result in the corrosion of strands in PT bridges (FDOT 1999) [18–20,2–4]. An external tendon consists of multiple strands placed inside a high-density-polyethylene (HDPE) duct. After post-tensioning, the interstitial spaces between the duct and strands are filled with cementitious grout for corrosion protection. Fig. 1(a) shows the cross-section of a tendon with no voids. However, due to bleed water evaporation and poor grouting practices [20,2,3,21–24], voids can form inside these ducts, especially at the anchorage regions, leaving the strands unprotected by the grout. If the tendon is damaged, the strand is directly exposed to the external environment, which in some cases can be aggressive. Fig. 1(b) shows the cross-sections of tendons with partial and full voids. Woodward [25] and Woodward et al. [26] reported the presence of voids with sufficient size to facilitate accelerated strand corrosion.

Based on the data in [28], it is concluded that approximately 12% of the external ducts had at least one opening (i.e., a damaged duct or an open hole in the system) through which chlorides or moisture from the outside environment can infiltrate the tendon system. The infiltrated chloride or moisture can collect inside the tendons making direct contact with the strands [26]. As soon as the strands come in direct contact with the infiltrated moisture or other deleterious elements, corrosion occurs. Gardoni et al. [29], Trejo et al. [30], and Pillai et al. [31] found that the void, chloride, and moisture conditions inside the tendon can significantly reduce the C_T of strands. It was also found that the prestressed strands exhibit increased strength reductions due to corrosive conditions as compared to unstressed strands.

2.2. Challenges in the estimation of applied normal stresses

Fig. 2 shows the cross-section at the midspan of an example PT bridge. The tendons numbered T1, T2, and T3 are external tendons. The remaining tendons are internal tendons. As mentioned earlier, this paper focuses on the effect of the corrosion of external tendons only on the service reliability (based on normal stresses) of PT bridges.

The AASHTO [32] and AASHTO LRFD Specifications [5] provide guidelines to calculate D_f for PT bridges. The use of these formulations during the design of PT bridges is straightforward; as the C_T of each strand is assumed to be constant. However, the C_T of strands in a PT bridge exposed to corrosive environments should be considered as a random variable; making the analysis process more complex. The corrosion-induced variations in the C_T of individual strands indicate variations among the cross-sectional area, A_{ps}, of individual strands. The variation in the available A_{ps} among the strands induces variations in the tensile forces among the strands and the neutral axis depth, c, of the girder cross section. In addition, the applied load is re-distributed as one or more strands fails. A probabilistic approach considering these complex mechanisms would provide a more realistic estimate of the D_f for segmental, PT bridges.

3. Modeling time-variant service reliability

The effect of the corrosion-induced loss in the C_T of external tendons on $\beta(\mathbf{x}, t)$ of existing PT bridges is the focus of this paper. Following conventional structural reliability theory [33], the service limit state function, $g(\mathbf{x}, t)$, is defined as follows:

$$g(\mathbf{x}, t) = C_f(\mathbf{x}) - D_f(\mathbf{x}, t) \tag{1}$$

such that the event $g(\mathbf{x}, t) < 0$ represents a service failure. Following the general expression for $g(\mathbf{x}, t)$ in Eq. (1), three service limit state functions, $g_{\text{compression},1}$, $g_{\text{compression},2}$, and g_{tension}, are defined as follows:

$$\begin{aligned} g_{\text{compression},1}(\mathbf{x}, t) &= C_{\text{compression},1}(\mathbf{x}) - D_{\text{compression},1}(\mathbf{x}, t) \\ g_{\text{compression},2}(\mathbf{x}, t) &= C_{\text{compression},2}(\mathbf{x}) - D_{\text{compression},2}(\mathbf{x}, t) \\ g_{\text{tension}}(\mathbf{x}, t) &= C_{\text{tension}}(\mathbf{x}) - D_{\text{tension}}(\mathbf{x}, t) \end{aligned} \tag{2}$$

where $C_{\text{compression},1}$ and $D_{\text{compression},1}$ represent the allowable and applied normal stresses, respectively, at the extreme fiber under dead load only; $C_{\text{compression},2}$ and $D_{\text{compression},2}$ represent the allowable and applied normal stresses, respectively, at the extreme fiber under dead and live loads; and C_{tension} and D_{tension} represent the allowable and applied normal stresses at the extreme fiber under dead and live loads. If any of the limit state functions (i.e., $g_{\text{compression},1}$, $g_{\text{compression},2}$, or g_{tension}) is less than zero, then service failure occurs (i.e., $g(\mathbf{x}, t) < 0$). The frameworks to probabilistically determine $C_f(\mathbf{x})$ and $D_f(\mathbf{x}, t)$ are discussed later. These frameworks and Eq. (2) are programmed in MATLAB® and incorporated into the reliability software FERUM [34] to determine $\beta(\mathbf{x}, t)$.

Fig. 3 shows a simplified flowchart of the process used in this research to determine β. In Fig. 3, the box with a thick border indicates the Monte Carlo simulation process used to determine the probability of service failure, P_f. The value of P_f after each simulation is calculated as the ratio of N_f and N_{sim}, which are the number of instances with service failure and the number of simulations, respectively. Then the approximate value of the coefficient of variation of P_f [i.e., COV(P_f)] is calculated as $[(1 - P_f)/(P_f N_{sim})]^{0.5}$ [33]. The simulation process is continued until COV(P_f) reaches a value less than or equal to a target value (i.e., COV$(P_f)_{\text{target}}$). Then the value of $\beta(\mathbf{x}, t)$ is determined as follows [33]:

$$\beta(\mathbf{x}, t) = -\Phi^{-1}(P_f) \tag{3}$$

where Φ is the cumulative distribution function (CDF) of the standard normal distribution. The probabilistic frameworks for $C_f(\mathbf{x})$ and $D_f(\mathbf{x}, t)$ are developed next.

3.1. Normal stress capacity

The AASHTO LRFD Specifications [5] prescribe maximum compressive and tensile stress limits for prestressed concrete bridge elements in service. These stress limits are independent of time and are based on the specified compressive strength of concrete, $f'_{c,\text{specified}}$. However, $f'_{c,\text{specified}}$ is replaced with actual compressive strength of concrete, f'_c, which is modeled as a random variable to capture the associated uncertainty. Therefore,

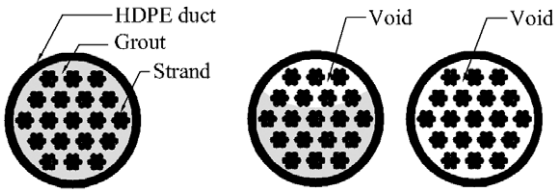

(a) Tendon with no voids. (b) Tendon with partial and full voids.

Fig. 1. Cross-sectional views of tendons without and with voids (after [27]).

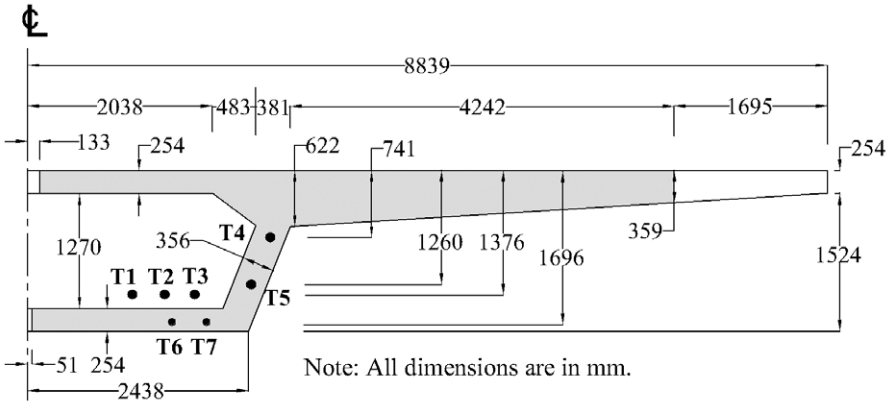

Fig. 2. Semi-cross-section at mid-span of a segmental, PT box girder (after [27]).

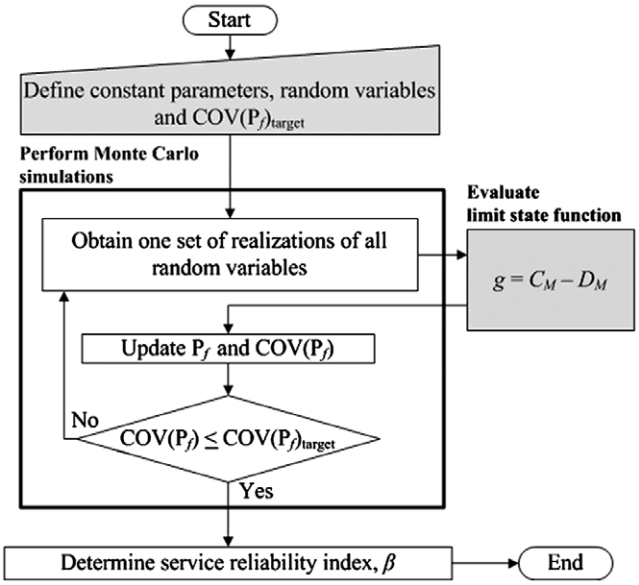

Fig. 3. Framework to determine the generalized reliability index, β (after [27]).

$C_{\text{compression},1}$, $C_{\text{compression},2}$, and C_{tension} are expressed as follows:

$$C_{\text{compression},1} = 0.45 f_c'$$
$$C_{\text{compression},2} = 0.60 \phi_w f_c' \quad (4)$$
$$C_{\text{tension}} = 0$$

where, ϕ_w is the stress limit reduction factor, which is calculated per AASHTO LRFD Specifications [5] and depends on the geometry and slenderness of a box section.

3.2. Normal stress demand

3.2.1. General

Estimating the normal stress at extreme fibers is straightforward when the strands are in "as-received" condition. However, the C_T of strands can decrease as a function of time and exposure conditions, resulting in changes in the effective prestress forces, P_e, in strands, which in turn induces changes in the normal stresses acting on the cross section. The moment demand, D_M, under service load conditions is a random variable. In addition, some realizations of D_M might be large enough such that some strands can break, especially if they are corroded. The effective prestress, f_{pe}, earlier imposed by the currently broken strands should be removed from further calculations of normal stresses. An iterative procedure, which considers these changes, has been developed to determine the probabilistic values for $D_{\text{compression},1}$, $D_{\text{compression},2}$, and D_{tension} [27,17]. The following is a discussion on this procedure.

3.2.2. Calculation of moment demand

At first, it is determined if the moment demand, D_M, is greater than the nominal moment capacity, C_M, of the PT girder. The dead, live, and impact loads are used in formulating D_M. The dead load due to the weight of the precast box section is denoted as DL_{box}. The combined dead load due to the weight of the overlay, future wearing surface, and side barriers is denoted as $DL_{\text{non-box}}$. The unit weights of the reinforced concrete used in these elements are denoted as ρ_{box} and $\rho_{\text{non-box}}$. In this paper, DL_{box} and $DL_{\text{non-box}}$ are expressed as uniformly distributed loads and are calculated using the span, cross-sectional geometry of the girder, ρ_{box}, and $\rho_{\text{non-box}}$. Following the procedures in the AASHTO Standard Specifications [35] and the AASHTO LRFD Specifications [5], the design lane (LL_{lane}), truck (LL_{truck}), and tandem (LL_{tandem}) loads are used to calculate the total live load for HS20 and HL93 loading conditions. Per AASHTO Standard Specifications [35], an impact load equal to (50/[125 + span in feet]) percent of live load is included for HS20 loading. Per AASHTO LRFD Specifications [5], an impact load equal to 33% of live load is included for HL93 loading. Herein, the symbol "*LL*" indicates the sum of the live and impact loads. Using structural mechanics principles and influence line theory, the critical section with the maximum value of bending moment is determined for the PT girder. The term D_M is then defined equal to this maximum bending moment. The uncertainty in D_M is captured

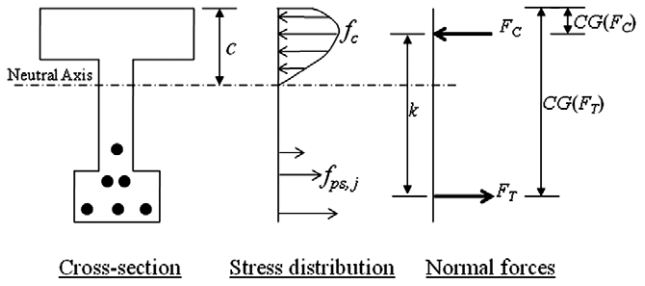

Fig. 4. Simplified cross-section of a box girder showing the stresses and forces (after [27]).

by modeling ρ_{box}, $\rho_{\text{non-box}}$, LL_{lane}, LL_{truck}, and LL_{tandem} as random variables.

3.2.3. Calculation of nominal moment capacity

The procedure to determine the nominal moment capacity, C_M, of a corroding PT girder follows a mechanics based sectional analysis approach similar to that provided in the AASHTO LRFD Specifications [5]. A typical PT girder can be represented by an equivalent T-section. Fig. 4 shows a schematic of a typical T-section with normal stresses and forces acting on the cross-section, which are referenced in the following discussion.

The normal compressive stress, f_c, in concrete is determined using the nonlinear stress–strain model for concrete by Todeschini et al. [36]. This model is used because it is a single closed-form solution, and hence, suitable for efficient numerical simulation. The maximum allowable compressive strain in concrete is assumed to be 0.003, per the AASHTO LRFD Specifications [5]. Following these, the total compressive force, F_C, on the concrete cross-section and its center of gravity, $\text{CG}(F_C)$, are determined.

The tensile force in each strand depends on the available A_{ps} of each strand and is critical to computing C_M. The A_{ps} for each strand is calculated as follows:

$$A_{ps,j} = C_{T,j}\left(\frac{A_{\text{as-received}}}{C_{T,\text{as-received}}}\right) \tag{5}$$

where the subscript j indicates the jth strand, $C_{T,j}$ is the C_T of the strand predicted using the probabilistic models by Trejo et al. [27], and $A_{\text{as-received}}$ and $C_{T,\text{as-received}}$ are the cross-sectional area and average C_T of "as-received" strand with negligible corrosion, respectively. The average stress at nominal conditions, $f_{ps,j}$, in each strand is calculated using the following expression for unbonded strands [5]:

$$f_{ps,j} = \underbrace{\left[f_{pe,j} + f_{\text{empirical}}\left(\frac{d_{p,j}-c}{l_e}\right)\right]}_{f_{ps,j,\text{calculated}}} \le f_{py}; \quad l_e = \left(\frac{2l_i}{2+N_s}\right) \tag{6}$$

where $d_{p,j}$ is the distance between the extreme compression fiber and centroid of the jth strand, l_e is the effective tendon length, l_i is the length of the strand between anchorages, N_s is the number of support hinges crossed by the strand between the anchorages, and f_{py} is the yield strength of strand. The value of the empirical constant, $f_{\text{empirical}}$, is 6200 and 900, when the units of stress variables (i.e., f_{pe} and f_{py}) are kN/mm^2 and ksi, respectively. The term f_{pe} is calculated by subtracting prestress losses at a given time due to long-term effects, Δf_{pLT}, from the initial prestress after anchoring, f_{pi}, as follows:

$$f_{pe,j} = f_{pi} - \Delta f_{pLT,j} = \frac{0.70 \times MUTS}{A_{\text{as-received}}} - \frac{P_{\text{loss,as-received},j}}{A_{\text{as-received}}} \tag{7}$$

where the subscript j indicates the jth strand; $P_{\text{loss,as-received},j}$ is the loss in prestress force on an "as-received" strand; and $MUTS$ is the minimum ultimate tensile strength of "as-received" strand with negligible corrosion. The value of $f_{ps,j,\text{calculated}}$ in Eq. (6) varies due to the change in c from one iteration to another. Finally, the tensile force in each strand, $F_{T,j}$, is equal to $A_{ps,j} \times f_{ps,j}$. Then, the total tensile force, F_T, acting on the cross-section and its center of gravity, $\text{CG}(F_T)$, are determined. Iterations are carried out with different values of curvature, ϕ, and different values of c. For each iteration, if equilibrium exists between F_C and F_T, the value of the bending moment, M, is calculated using the moment arm, k, and F_T. The maximum of all the determined values of M is defined as C_M.

3.2.4. Calculation of normal stress demand

If D_M is greater than C_M, then the girder fails in flexure and $g(\mathbf{x}, t)$ is assumed to be negative; indicating service failure. If D_M is less than or equal to C_M, then further calculations are needed to determine the value of $g(\mathbf{x}, t)$ per Eq. (2). The terms $D_{\text{compression},1}$, $D_{\text{compression},2}$, and D_{tension} in Eq. (2) are determined as follows for the case when the strands are below the center of gravity of the cross section and the external moments cause tension in the extreme bottom fibers at the cross section considered [37–39]:

$$\begin{aligned}
D_{\text{compression},1} &= \sum_{j=1}^{N_{\text{strands}}}\left[-\frac{P_{e,j}}{A_c}\left(1-\frac{e_j c_t}{r^2}\right)\right] - \left(\frac{D_{M,DL}}{S^t}\right)\\
D_{\text{compression},2} &= \sum_{j=1}^{N_{\text{strands}}}\left[-\frac{P_{e,j}}{A_c}\left(1-\frac{e_j c_t}{r^2}\right)\right] - \left(\frac{D_{M,DL}+D_{M,LL}}{S^t}\right)\\
D_{\text{tension}} &= \sum_{j=1}^{N_{\text{strands}}}\left[-\frac{P_{e,j}}{A_c}\left(1+\frac{e_j c_b}{r^2}\right)\right] + \left(\frac{D_{M,DL}+\gamma_{\text{load}}D_{M,LL}}{S_b}\right)
\end{aligned} \tag{8}$$

where, $P_{e,j}$ is the effective prestress force in the jth strand after losses; N_{strands} is the total number of strands in the cross section; e is the eccentricity of each strand from the center of gravity of the concrete cross section; r is the radius of gyration; A_c is the concrete's cross sectional area; $D_{M,DL}$ is the moment demand due to dead load only; and $D_{M,LL}$ is the moment demand due to live and impact loads; S^t and S_b are section moduli of concrete sections with reference to the extreme top and bottom fibers, respectively; c_t and c_b are the distances to the extreme top and bottom fibers, respectively, from the centroid of the concrete cross section; and the term γ_{load} is 1.0 and 0.8, when HS20 and HL93 loadings, respectively, are considered. The γ_{load} for HL93 loading is defined based on the live load factor for the Service III limit state (Table 3.4.1-1 of [5]).

The effective prestress force in a given strand, $P_{e,j}$, is equal to $A_{ps,j} \times f_{pe,j}$ for uncorroded, partially corroded, and unbroken strands, and is zero for completely corroded or broken strands. The value of $A_{ps,j}$ is determined using Eq. (5), which considers the effect of corrosion. For a completely corroded strand, $A_{ps,j}$ is zero; therefore, $P_{e,j}$ will also be zero. However, it is also necessary to determine whether each strand is broken or not. For a given D_M, the corresponding value of c is computed by meeting the criteria $M = D_M$ and then substituted in Eq. (6) to determine the total stress in each strand. If $f_{ps,j,\text{calculated}}$ is greater than the ultimate tensile stress capacity of strand, f_{pu}, then the strand fails in tension (i.e., broken) and is removed from further calculations by setting the corresponding $A_{ps,j}$ and $P_{e,j}$ to zero. If $f_{ps,j,\text{calculated}}$ is between f_{py} and f_{pu}, then $f_{ps,j}$ is set equal to f_{py} (per the limit in Eq. (6)).

4. Random variables influencing service reliability

4.1. Structural load parameters

The random variables associated with the dead load parameters, DL_{box} and $DL_{\text{non-box}}$, are the unit weights of the corresponding

reinforced concrete materials (i.e., ρ_{box} and $\rho_{\text{non-box}}$). Because ρ_{box} and $\rho_{\text{non-box}}$ are always positive, they can be assumed to be independent and follow lognormal distributions. The mean of ρ_{box} is assumed to be 25 kN/m^3 (155 lb/ft^3) and that of $\rho_{\text{non-box}}$ is assumed to be 24 kN/m^3 (150 lb/ft^3). The standard deviations of ρ_{box} and $\rho_{\text{non-box}}$ are obtained based on a COV of 0.10 [6].

The mean values of live load parameters, LL_{lane}, LL_{truck}, and LL_{tandem}, are determined using the standard procedures provided in the AASHTO Standard Specifications [35] for HS20 loading and the AASHTO LRFD Specifications [5] for HL93 loading conditions. Per Nowak and Collins [6], live loads can be modeled as normal distributions with a bias factor and COV of 1.25 and 0.18 for the joint effect of live and impact loading.

4.2. Compressive strength of concrete

The term f_c' is a positive number and is expressed as a lognormal distribution. The COV of f_c' can be assumed to be 0.15 [6] and the corresponding standard deviation can be determined.

4.3. Void and damage/opening conditions

The void condition and the damage condition are defined on the basis of the probability of the presence of a voided tendon (P_{VT}) and the probability of the presence of a damaged tendon (P_{DT}). A tendon with at least one void is considered as a voided tendon. A damaged tendon is defined as a tendon with at least one unsealed hole or vent at the anchorage region or any damage to the tendon that allows the ingress of water or aggressive ions into the duct. As Woodward [25] and Woodward et al. [26] determined, P_{VT} can be determined based on inspection of sample bridges or tendons or assumed based on sound engineering judgment. Similarly, P_{DT} can be determined or assumed. The two void conditions considered are 'no void' and 'void' conditions. The two damage conditions considered are 'no damage' and 'damaged' conditions. Therefore, the void condition and damage condition are modeled as binomial distributions using P_{VT} and P_{DT} as model parameters (i.e., success probabilities). Based on the data from [28], P_{VT} and P_{DT} are calculated to be 78.6% and 12%, respectively.

4.4. Tension capacity of strands

Trejo et al. [27] and Pillai et al. [31] developed probabilistic models to predict the C_T of strands subjected to stress and different void conditions and environmental conditions. The environmental conditions included relative humidity (RH), temperature (T), and chloride concentration in the grout and infiltrated solution ($\%gCl^-$ and $\%sCl^-$, respectively). Among these, the following four models are used to assess the $\beta(\mathbf{x}, t)$ of PT bridges.

$$\text{Model 1: } C_T \sim MUTS \times \text{Lognormal}\,(1.011, 0.0049) \tag{9}$$

$$\text{Model 2: } C_T = MUTS \times \left[A\left(h_{t_{CA}}\right)^{n_{CA}} + \sigma\varepsilon\right] \quad \text{where,}$$

$$A = \theta_1\left\{\theta_2 - \theta_3 \exp\left(h_{RH}\right) - \theta_4 \exp\left[h_{\%gCl^-} \exp\left(h_{RH}\right) h_T\right]\right\}^{\theta_5} \tag{10}$$

$$\text{Model 3: } C_T = MUTS \times \left[\theta_1\left(\theta_2 - \theta_3 h_{\%sCl^-} h_{t_{WD}}\right)^{\theta_4} + \sigma\varepsilon\right] \tag{11}$$

Model 4:

$$C_T = MUTS \times \left[\theta_1\left(\theta_2 - \theta_3 h_{t_{WD}} - \theta_4 \ln[h_{\%sCl^-}] h_{t_{WD}}\right)^{\theta_5} + \sigma\varepsilon\right]. \tag{12}$$

Table 1 shows the definitions of the explanatory functions or predictor variables (i.e., h_{RH}, h_T, $h_{\%sCl^-}$, $h_{\%gCl^-}$, $h_{t_{WD}}$, $h_{t_{CA}}$). Table 2 shows the mean estimates and standard deviations of the unknown model parameters (i.e., θ_i and σ). Trejo et al. [27] provides further details on the correlation coefficients of these models. The probabilistic model for the C_T of each strand is selected based on the tendon type (i.e., external or internal tendon) and the pre-defined environmental condition and the randomly selected void condition and damage condition.

Table 1
Definitions of the terms in the strand capacity models.

Terms	Definitions
θ_i	Unknown model parameter
σ	Standard deviation of model error
ε	Standard normal variable ~Normal (0, 1)
$h_{t_{CA}}$	$\frac{\text{Total atmospheric exposure time (years)}}{\text{standardizing factor}} = \frac{t_{CA}}{0.75}$
n_{CA}	Constant based on field information $= -0.005$
h_T	Ambient exposure temperature (°F) $= T$ (°F)
h_{RH}	$\frac{\text{Ambient relative humidity (\%)}}{\text{Maximum relative humidity (\%)}} = \frac{RH\ (\%)}{100}$
$h_{\%gCl^-}$	$\frac{\%Cl^-\text{ in the grout (by weight)}}{\%sCl^-_{\text{saturated chloride solution}}} = \frac{\%gCl^-}{35.7}$
$h_{\%sCl^-}$	$\frac{\%Cl^-\text{ in the water inside the tendon}}{\%sCl^-_{\text{saturated chloride solution}}} = \frac{\%sCl^-}{35.7}$
ϕ_{wet}	$\left(\frac{\text{Wet-time in a year (months)}}{12\text{ (months)}}\right);\ 0 \le \phi_{\text{wet}} \le 1$
$h_{t_{WD}}$	$\phi_{\text{wet}} \times \text{Total exposure time (years)} = \phi_{\text{wet}} \times t_{WD}$

Note: °F = (°C × 9/5) + 32.

Table 2
Mean estimates of model parameters in the strand capacity models.

Model parameters	Model 2	Model 3	Model 4
θ_1	7.7492 (0.9532)	0.9983 (0.0014)	0.9463 (0.0064)
θ_2	0.1637 (0.0018)	1.0105 (0.0022)	1.0333 (0.0056)
θ_3	0.0030 (0.0008)	1.6785 (0.1362)	0.3567 (0.0648)
θ_4	0.0002 (0.0000)	1.3576 (0.0648)	0.0285 (0.0015)
θ_5	1.0924 (0.0617)	–	2.0301 (0.0773)
σ	0.0619 (0.0047)	0.0117 (0.0011)	0.0350 (0.0107)

The values in parenthesis indicate standard deviations.

Fig. 5 shows the methodology used to select the probabilistic models to determine the C_T of strands, where the circles indicate the model number for each exposure category. The environmental condition can be manually selected per the user's choice. The user can make approximate estimations on the environmental exposure parameters (such as moisture and chloride exposure levels) based on (1) the databases available with the National Climatic Data Center, (2) laboratory tests on field samples, and (3) suitable engineering judgments based on experience. The void condition and damage condition are randomly realized as explained before. The two void conditions considered are "no void" and "void" conditions. The two damage conditions considered are "no damage" and "damaged" conditions. During a rainy season, a damaged tendon can become infiltrated with water and experience a wet condition. The wet tendon can naturally dry over a period of time. This cyclic process during the life of a bridge can be defined as a "wet–dry" condition (based on the average wet-time and dry-time in a year). Further details on "wet–dry" conditions are provided in [27]. Because the "wet–dry" condition inside the tendons can occur only if there is damage on the tendon system, the combination of "no damage" and "wet–dry" conditions does not exist and is not shown in Fig. 5.

4.5. Prestress loss of strands

The $P_{\text{loss,as-received}}$ for each strand, which is used in Eq. (7) is assumed to follow a lognormal distribution as follows:

$$P_{\text{loss,as-received}} \sim A_{\text{as-received}} \times \text{Lognormal}\left[\overline{\Delta f}_{pLT}, \overline{\Delta f}_{pLT} \times \text{COV}\left(\Delta f_{pLT}\right)\right] \tag{13}$$

where $\overline{\Delta f}_{pLT}$ and $\text{COV}\left(\Delta f_{pLT}\right)$ are the mean and COV of Δf_{pLT}. The value of $A_{\text{as-received}}$ for a 15 mm (0.6-inch) diameter PT strand is 140 mm^2 (0.217 inch^2). The value of $\overline{\Delta f}_{pLT}$ is assumed to be

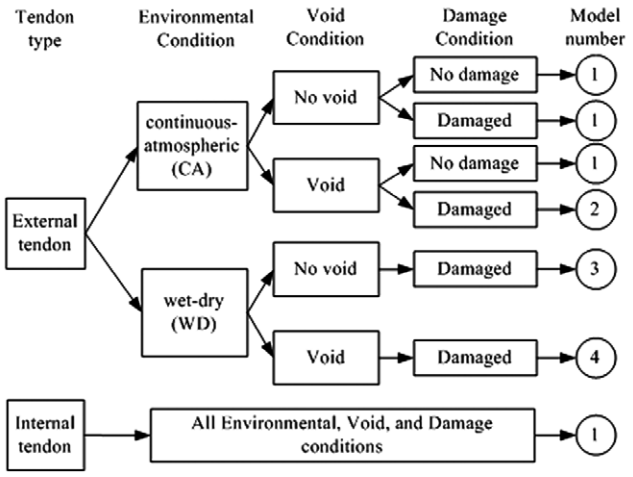

Fig. 5. Method to select the strand capacity models (after [27]).

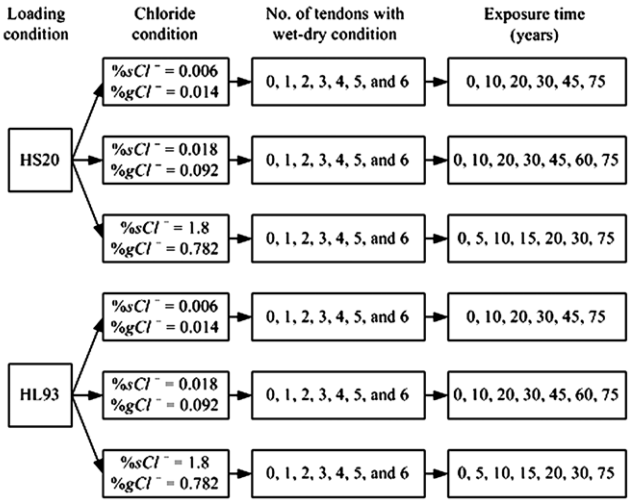

Other parameters: Ambient RH = 70%, RH inside undamaged tendons = 50%, T = 70°F (24.4 °C), ϕ_{wet} = 2/12 = 0.17, n_{CA} = − 0.005

Fig. 6. Constant parameter combinations for the reliability assessment.

131 MPa (19,000 psi), which is the AASHTO LRFD [5] specified lump sum estimate of $\overline{\Delta f}_{pLT}$ in box girders; and the COV $\left(\Delta f_{pLT}\right)$ is assumed to be 0.15. In this way, the mean and standard deviation of $P_{\text{loss,as-received}}$ are calculated to be 18 kN (4123 lbs) and 2.8 kN (618 lbs), respectively.

5. Example: application of the service reliability framework

5.1. Description of example for PT bridge and parameter combinations

Fig. 2 shows one half of the symmetric cross-section of a representative PT girder, with the shaded region indicating the effective cross-section, per AASHTO LRFD Specifications [5]. The figure also shows the locations of 6 external and 8 internal tendons at the midspan of the girder. The tendons T1 through T5 contain 19 strands each and the internal tendons T6 and T7 contain 12 strands each. All the strands meet the ASTM A416 Specifications [40] and are 15 mm (0.6 inches) in nominal diameter. The PT girder is assumed to be simply supported with a clear span of 30.5 m (100 ft).

Fig. 6 shows the pre-defined combinations of parameters used in the reliability assessment. The two loading conditions (i.e., HS20 and HL93), three chloride conditions (based on $\%sCl^-$ and $\%gCl^-$ levels), and 0 through 6 external tendons with wet–dry conditions are considered. The external tendons without wet–dry conditions will be assumed to have a continuous-atmospheric condition. All internal tendons are assumed to be free from corrosion. The fourth column in Fig. 6 shows the values of t, at which $\beta(\mathbf{x}, t)$ will be determined. These values of t are selected such that a better estimation of intermediate values of $\beta(\mathbf{x}, t)$ can be obtained, especially when $\beta(\mathbf{x}, t)$ changes rapidly as a function of t.

5.2. Time-variant service reliability index

Using the developed framework, this paper determines the values of $\beta(\mathbf{x}, t)$ of the selected PT bridge. Table 3 summarizes the definitions of all the random variables used in obtaining the values of $\beta(\mathbf{x}, t)$. The $\text{COV}(P_f)_{\text{target}}$ was set to 0.01 for this analysis. The ISO (2001) recommends β_{target} values of 0 and 1.5 (corresponding to P_f of 0.50 and 0.07) for service failures with reversible and irreversible consequences. Although there are concrete materials that can self-heal microcracks, standard concrete materials generally exhibit crack formation that will not self-heal when stresses exceed the tensile stress limit. Such cases could be defined to have an irreversible consequence of failure. In addition, exceeding the compressive stress limits generally results in inelastic stresses and this could also be considered to have irreversible consequences. Although not typical, there may also be cases with reversible consequences of failure (such as in the cases of concrete capable of self-healing tensile cracks or elastic behavior beyond the compressive stress limit). The following subsections compare the estimated $\beta(\mathbf{x}, t)$ with the ISO (2001) recommended β_{target} values for service failures.

5.2.1. Service reliability when strands are in "as-received" condition

For the selected PT bridge, $\beta(\mathbf{x}, t)$ is below 1.5 and above 0 when the strands are in "as-received" condition (i.e., when $t = 0$). In particular, the values of $\beta(\mathbf{x}, t)$ are 1.22 and 0.63, when the bridge is subjected to HS20 and HL93 loadings, respectively. Note that these values are specific to the typical PT bridge defined in this paper. The corresponding values of $\beta(\mathbf{x}, t)$ for an actual PT bridge could be different from these values and the values presented in the following discussions.

5.2.2. Service reliability when strands are exposed to various chloride solution

Fig. 7(a)–(c) show the variation of $\beta(\mathbf{x}, t)$ with time when exposed to 0.006, 0.018, and 1.8 $\%sCl^-$ solutions, respectively. The horizontal lines with long dashes indicate the values of β_{target} suggested by ISO (2001) for service failures with reversible and irreversible consequences. The dashed curves (with hollow data markers) and solid curves (with solid data markers) indicate HS20 and HL93 loading conditions, respectively. Different data markers are used to represent the number of tendons subjected to wet–dry exposure cycles (denoted as WDT in Fig. 7).

Fig. 7(a) shows the variation of $\beta(\mathbf{x}, t)$ with time when exposed to a 0.006 $\%sCl^-$ solution. When there is only one tendon with wet–dry exposure and the bridge is subjected to HS20 loading (hollow round markers), the predicted value of $\beta(\mathbf{x}, t)$ is below 1.5 and above 0 for up to 75 years. For this case, when the bridge is subjected to HL93 loading (solid round markers), the value of $\beta(\mathbf{x}, t)$ stays above 0 for approximately 25 years. When there are two tendons with wet–dry exposure (square markers), these time estimates reduce to about 25 and 10 years, respectively. If the bridge is subjected to HS20 loading and there are three or more tendons with wet–dry exposure (all hollow triangular markers), then the time needed for $\beta(\mathbf{x}, t)$ to drop below 0 is between 7 and

Table 3
Random variables for reliability assessment.

Random variables	Distribution (mean, standard deviation)
Void condition	~Binomial (0.79, 0.407)
Damage condition	~Binomial (0.12, 0.325)
Error term in the strand capacity model, ε	~Normal (0, 1)
Prestress loss of "as-received" strand, $P_{\text{loss,as-received}}$	~Lognormal (18 300, 2700) kN
Compressive strength of concrete, f'_c	~Lognormal (41.3, 6.2) MPa
Unit weight of concrete in the box girder, ρ_{box}	~Lognormal (2500, 250) kg/m^3
Unit weight of concrete in overlay, future wearing surface, and side barriers, $\rho_{\text{non-box}}$	~Lognormal (2400, 240) kg/m^3
Live load due to multiple lane load, LL_{lane}	~Normal (7.3, 1.5) kN/m
Live load due to design truck load, LL_{truck}	~Normal (1115, 20) kN
Live load due to design tandem load, LL_{tandem}	~Normal (89, 16) kN

Notes: 1 kN = 0.225 kips; 1 MPa = 0.145 ksi; 1 kg/m^3 = 0.062 lbs/ft^3; 1 kN/m = 0.068 kip/ft.

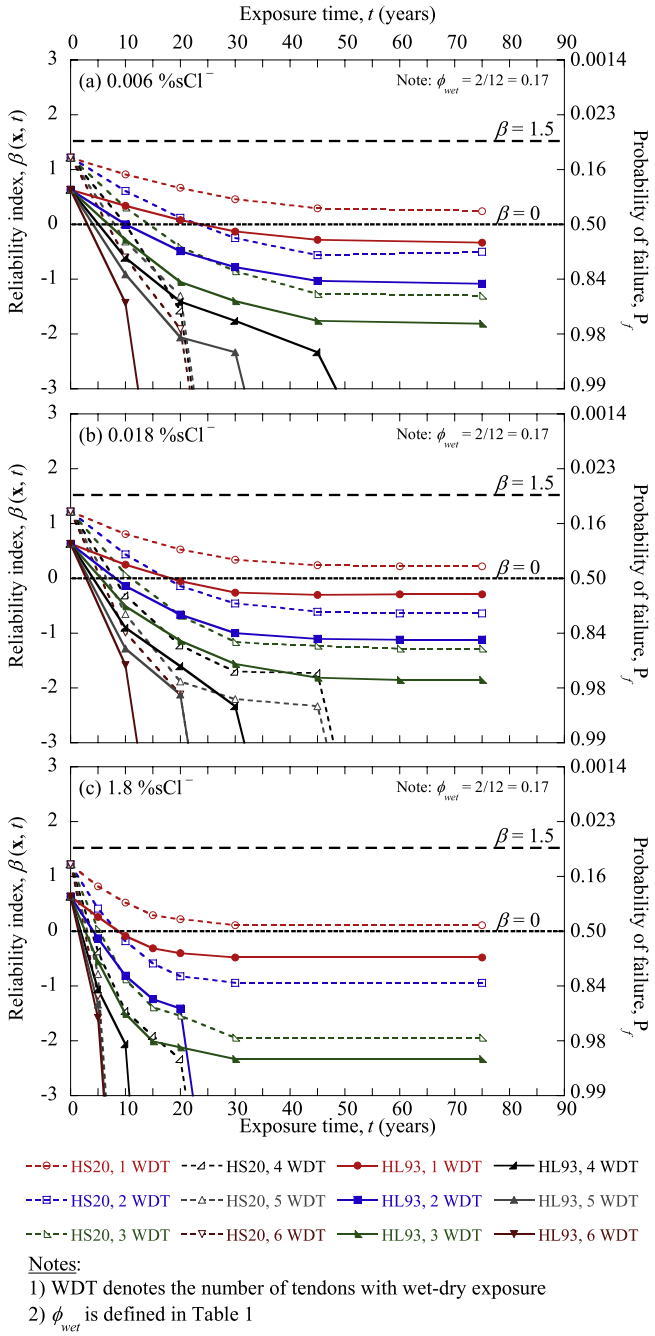

Fig. 7. Time-variant service reliability of the typical PT bridge.

15 years. If the bridge is subjected to HL93 loading and there are three or more tendons with wet–dry exposure (all solid triangular markers), then the time needed for $\beta(\mathbf{x}, t)$ to drop below 0 is between 3 and 5 years. The quick drop in the curves corresponding to four or more tendons with wet–dry exposure is because $\beta(\mathbf{x}, t)$ quickly reached −8.21 (i.e., P_f reached 1). Similar occurrences in Fig. 7(b) and (c) are not discussed herein. Fig. 7(b) and (c) show the variations in $\beta(\mathbf{x}, t)$ with time when exposed to 0.018 and 1.8 $\%sCl^-$ solutions, respectively. In general, the time estimates are less than the time estimates when exposed to 0.006 $\%sCl^-$ solution. Table 4 summarizes the major time estimates from Fig. 7(a)–(c).

Table 4
Approximate time (in years) required for $\beta(\mathbf{x}, t)$ to reach zero.

Loading condition	$\%sCl^-$	Number of external tendons with wet–dry conditions			
		1	2	3	6
HS20	0.006	>75	25	15	7
	0.018	>75	18	13	6
	1.8	>75	9	5	2
HL93	0.006	25	10	5	3
	0.018	20	9	7	3
	1.8	9	4	4	2

6. Conclusions

This paper developed an analytical framework to predict the time-variant service reliability index, $\beta(\mathbf{x}, t)$, of post-tensioned (PT), segmental concrete bridges subjected to various structural loading and corrosive exposure conditions. The service reliability framework evaluates the applied normal stresses (demand) at the extreme fibers of the PT girder section at the location of the maximum moment in service and compares these stresses to the normal stress limits (capacity) provided in the AASHTO LRFD Specifications [5]. The developed framework accounts for (1) the uncertainties in the tension capacity and prestress loss, void condition and damage condition of tendons, the compressive strength and unit weight of concrete, and live load conditions, (2) the effects of different levels of corrosion-induced loss in the tension capacity of strands, and (3) the re-distribution of loads upon tension failure or complete corrosion of a strand.

An example PT bridge was defined to demonstrate the application of the developed service reliability framework. The example bridge includes a single box girder section with a 30.5 m (100 ft) span and simply supported end conditions. For this application example, only selected external tendons were assumed to be exposed to corrosive conditions, while all internal tendons were assumed to be intact and free from corrosion. The following conclusions are drawn based on development of the service reliability model for PT bridges and the application example provided:

- The value of $\beta(\mathbf{x}, t)$ can be estimated and used as a serviceability indicator for PT bridges provided that appropriate deterioration models are incorporated to account for potential strand corrosion.

- When the example PT bridge is subjected to HS20 or HL93 loading and all strands are in "as-received" condition, the reliability models estimates β values between 0 and 1.5, which are the β_{target} values recommended by ISO 13822 (2001) for service failures with reversible and irreversible consequences, respectively.
- When the example PT bridge is subjected to HS20 loading and only one tendon is exposed to wet–dry cycles with 0.006, 0.018, or 1.8 $\%sCl^-$ solutions, the reliability models show that β stays above 0 for more than 75 years.
- When the example PT bridge is subjected to HL93 loading and only one tendon is exposed to wet–dry cycles with 0.006 $\%sCl^-$ solution, β can drop to a value below 0 within about 25 years. This time estimate reduces to about 9 years when exposed to 1.8 $\%sCl^-$ (similar to seawater chloride concentration) solution.
- The service reliability index reduces significantly if more than one tendon in the example bridge is exposed to wet–dry cycles and falls below the β_{target} values recommended by ISO 13822 (2001) in a relatively short time frame.

The results demonstrate that these calculations, although computationally intensive, can be readily performed with current technology. In addition, the results underscore the importance of quality control in the initial construction of PT girders, along with ongoing inspection and maintenance programs to reduce the potential for strand corrosion in PT ducts.

Additional research to incorporate the various support conditions and erection sequences of segments, develop more precise probabilistic models for the long-term prestress losses, and address other service limit states (such as deflection criteria) to the developed reliability framework is recommended. In this paper, a box girder is simplified as a T-section, requiring an assumption that the tendons fail symmetrically and that the loading is symmetric. This may result in an overestimation of the reliability indices. More detailed models to predict the reliability indices could be developed using three-dimensional models that consider unsymmetrical load and resistance behavior. In addition, the example on the application of the reliability framework presented in this paper considers various constants for the environmental exposure parameters (moisture and chloride exposure levels). Developing time-variant statistical distributions for these environmental exposure parameters and then, re-assessing the time-variant structural reliability is a potential area for future research.

Acknowledgements

This research was performed at the Texas Transportation Institute and the Zachry Department of Civil Engineering, Texas A&M University, College Station, Texas, through a sponsored project from the Texas Department of Transportation and the Federal Highway Administration. This support is much appreciated. Continuous support from Jaime Sanchez (Project Director I), Maxine Jacoby (Project Director II), Dr. German Claros (Project Director III), Brian Merrill (Project Director IV), Keith Ramsey (Program Co-ordinator), Dean Van Landuyt, Kenneth Ozuna, Steve Strmiska, Tom Rummel, and other TxDOT engineers is acknowledged. The authors also acknowledge the assistance from Dr. Daren Cline, Ramesh Kumar, and Byoung Chan Jung during this research.

References

[1] FDOT. 1999. Corrosion evaluation of post-tensioned tendons on the Niles Channel Bridge. Florida Department of Transportation (FDOT), Tallahassee, Florida.
[2] FDOT. 2001. Mid-Bay bridge post-tensioning evaluation – final report. Washington (DC): Corven Engineering, Inc., Florida Department of Transportation (FDOT), Tallahassee, Florida.
[3] FDOT. 2001. Sunshine skyway bridge post-tensioned tendons investigation. Parsons Brinckerhoff Quade and Douglas, Inc., Florida Department of Transportation (FDOT), Tallahassee, Florida.
[4] Hansen B. Forensic engineering: tendon failure raises questions about grout in post-tensioned bridges. Civil Eng News 2007;November:17–8.
[5] AASHTO. LRFD bridge design specifications. 4th ed. Washington (DC): Association of State Highway and Transportation Officials (AASHTO); 2007.
[6] Nowak AS, Collins KR. Reliability of structures. Boston (MA): McGraw-Hill Companies, Inc.; 2000.
[7] AASHTO. LRFD bridge design specifications. 2nd ed. Washington (DC): Association of State Highway and Transportation Officials (AASHTO); 1998.
[8] CDCHB. Chinese design code for highway bridges. Beijing (China): People's Communication Press; 1991.
[9] SDMHR. 1997. Structures design manual for highways and railways. Highways Department, Government of the Hong Kong Special Administrative Region. 2nd ed., with Amendment No. 1/2002, Hong Kong.
[10] Du JS, Au FTK. Deterministic and reliability analysis of prestressed concrete bridge girders: comparison of the Chinese, Hong Kong, and AASHTO LRFD codes. Struct Safety 2005;(27):230–45.
[11] Wassef WG. 2009. Calibration of LRFD concrete bridge design specifications for serviceability, NCHRP Project 12-83 [Active Project]. Austin (TX, USA): Modjeski & Masters, Inc., National Cooperative Highway Research Program (NCHRP), Transportation Research Board, National Research Council.
[12] Galambos TV, Ellingwood B. Serviceability limit states: Deflection. ASCE J Struct Eng 1996;112(1):67–84.
[13] Foschi RO, Folz BR, Yao FZ. 1989. Reliability-based design of wood structures. In: Structures research series report, vol. 34, Vancouver (BC, Canada): Department of Civil Engineering, University of British Columbia.
[14] Philpot TA, Rosowsky DV, Fridley KJ. Serviceability design in LRFD for wood. ASCE J Struct Div 1993;105(5):3649–67.
[15] Stewart MG. Serviceability reliability analysis of reinforced concrete structures. ASCE J Struct Eng 1996;122(7):794–803.
[16] Pillai RG, Trejo D, Gardoni P, Hueste MD, Reinschmidt FK. 2009. Time-variant flexural reliability of post-tensioned, segmental, concrete bridges exposed to corrosive conditions. Struct Safety [submitted for publication].
[17] Pillai RG. 2009. Electrochemical characterization and time-variant structural reliability assessment of post-tensioned, segmental concrete bridges. Ph.D. dissertation. College Station (TX, USA): Zachry Department of Civil Engineering, Texas A&M University.
[18] TRRL. 1987. Seventh report of the committee for the two years ending July 1987. EA/88/4. Crowthorne (United Kingdom): Standing Committee on Structural Safety, Transport and Road Research Laboratory (TRRL).
[19] NCHRP. 1998. Durability of precast segmental bridges. NCHRP Web Document No. 15, Project 20-7/Task 92. Washington (DC): National Cooperative Highway Research Program (NCHRP), Transportation Research Board, National Research Council.
[20] ASBI. American segmental bridge institute grouting committee: Interim statement on grouting practices. Phoenix (AZ): American Segmental Bridge Institute (ASBI); 2000.
[21] Schupack M. Grouting tests on large PP tendons for secondary nuclear containment structures. PCI J 1971;16(2):85–97.
[22] Schupack M. Admixture for controlling bleed in cement grout used in post-tensioning. PCI J 1974;16(2):28–39.
[23] Schupack M. Durability study *of a* 35-year-old post-tensioned *bridge*. Concr Int 1994;16(2):54–8.
[24] Schupack M. PT grout: Bleedwater voids. Concr Int 2004;26(8):69–77.
[25] Woodward RJ. 1981. Conditions within ducts in post-tensioned prestressed concrete bridges. LR 980. Crowthorne (Berkshire, United Kingdom): Transport and Road Research Laboratory, Department of Transport.
[26] Woodward R, Cullington D, Lane J. Strategies for the management of post-tensioned concrete bridges. In: Current and future trends in bridge design, construction, and maintenance 2: safety, economy, sustainability, and aesthetics. Hong Kong: Thomas Telford; 2001. p. 23–32.
[27] Trejo D, Hueste MD, Gardoni P, Pillai RG, Reinschmidt K, Kataria S. et al. 2009. Effects of voids in grouted, post-tensioned, concrete bridge construction. Report No. 0-4588-1. Austin (TX, USA): Transportation Institute, Texas Department of Transportation. URL: http://tti.tamu.edu/documents/0-4588-1-Vol1.pdf.
[28] TxDOT. 2004. Critical evaluation and condition assessment of post-tensioned bridges in Texas — final report. Austin (TX): Texas Department of Transportation.
[29] Gardoni P, Pillai RG, Trejo D, Hueste MD, Reinschmidt K. Probabilistic capacity models for corroding posttensioning strands calibrated using laboratory results. ASCE J Eng Mech 2009;135(9):906–16.
[30] Trejo D, Pillai RG, Hueste MD, Reinschmidt K, Gardoni P. Parameters influencing corrosion and tension capacity of post-tensioning strands. ACI Mater J 2009;106(2):144–53.
[31] Pillai RG, Gardoni P, Trejo D, Hueste MD, Reinschmidt K. 2009. Probabilistic models for the tensile strength of corroding strands in post-tensioned, segmental concrete bridges, ASCE J Mater Civil Eng [submitted for publication].
[32] AASHTO. Guide Specifications for design and construction of segmental concrete bridges. 2nd ed. Washington (DC): American Association of State Highway and Transportation Officials (AASHTO); 1999.
[33] Ditlevsen O, Madsen OH. Structural reliability methods, Chichester (UK): John Wiley & Sons Ltd.; 1996.
[34] Der Kiureghian A, Haukaas T, Fujimura A. Structural reliability software at the University of California, Berkeley. Struct Safety 2006;28(1–2):44–67.

[35] AASHTO. Standard Specifications for highway bridges. 17th ed. Washington (DC): Association of State Highway and Transportation Officials (AASHTO); 2002.
[36] Todeschini CE, Bianchini AC, Kesler CE. Behaviour of concrete columns reinforced with high strength steels. ACI J 1964;61–67:701–16.
[37] PCI. PCI design handbook. Chicago (Illinois): Precast/Prestressed Concrete Institute (PCI); 1999.
[38] Nawy EG. Prestressed concrete — A fundamental approach. Saddle River (New Jersey): Prentice Hall; 2003.
[39] Naaman AE. Prestressed concrete analysis and design. Ann Arbor (Michigan): Techno Press; 2004.
[40] ASTM A416. Standard specification for steel strand, uncoated-wire for prestressed concrete. Conshohoken, PA: American Society of Testing and Materials; 2002.